

## ***FUZZY GENETIC PARTICLE SWARM OPTIMIZATION CONVOLUTION NEURAL NETWORK BASED ON ORAL CANCER IDENTIFICATION SYSTEM***

**R. Dharani<sup>1</sup>, S. Revathy<sup>2\*</sup>, K. Danesh<sup>3</sup>**

Department of Information Technology, Panimalar Engineering College, Chennai, Tamilnadu, India<sup>1</sup>

School of Computing, Sathyabama Institute of Science and Technology, Chennai, Tamilnadu, India<sup>2</sup>

Department of ECE, SRM Institute of Science and Technology, Ramapuram Campus, Chennai, Tamilnadu, India<sup>3</sup>

dharanir.pec@gmail.com, ramesh.revathy@gmail.com, danesh.kn1@gmail.com

Received : 31 July 2023, Revised: 14 October 2023, Accepted : 21 October 2023

*\*Corresponding Author*

---

### **ABSTRACT**

*Oral cancer presents a pressing global health concern, ranking as the eighth most prevalent cancer worldwide and leading to a significant number of deaths, particularly evident in India with an annual toll of around 130,000 lives lost to mouth cancer. The urgency for early detection is evident, as delays in disease identification due to clinical exams and biopsies by skilled doctors can hinder effective treatment and improved patient outcomes. This study addresses this critical need through the development of a system capable of recognizing disease-affected oral regions and accurately classifying various oral cancer disorders. The research leverages Deep Learning algorithms to detect and precisely localize affected areas within oral images, incorporating advanced feature extraction techniques, notably pattern-based features. The innovative Bee Pulse Couple Neural Network (BeePCNN) algorithm is employed for effective segmentation of the affected regions. To further enhance detection efficiency, a novel Fuzzy Genetic Particle Swarm Convolutional Neural Network (FGPSOCNN) is introduced, reducing the computational complexity while preserving a high accuracy level. The proposed system undergoes rigorous evaluation using real-time MRI images gathered from Arthi Scan Hospital. The experimental results convincingly demonstrate the superiority of the FGPSOCNN model compared to existing oral cancer detection methods. This comprehensive study not only addresses the crucial need for early oral cancer detection but also introduces an innovative approach that significantly improves efficiency without compromising accuracy. The potential impact of this research on oral cancer diagnosis is substantial, offering a promising solution to a critical global health challenge.*

**Keywords:** *Oral cancer, Deep learning, BeePCNN, Fuzzy, Particle swarm optimization, FGPSOCNN.*

### **1. Introduction**

Oral cancer presents a significant global burden, both economically and in terms of clinical impact. Among the various forms of oral cancer, oral squamous cell carcinoma (OSCC) is the most common, accounting for about 90% of cases. (Ezhilarasan et al., 2022; Shamala et al., 2023; Zhou et al., 2023). OSCC originates from the squamous cells that line the oral cavity and is recognized for its aggressive behaviour, being prevalent among individuals with oral cancer. Fukumoto et al., (2022). Despite advancements in treatment, the 5-year survival rates for affected patients have remained stagnant due to delayed diagnosis. According to a report from the World Health Organization, the mortality rate for oral cancer within 5 years of diagnosis, considering all stages of diagnosis, stands at 45% (Mercadante et al., 2022). However, when the disease is identified early in its development, the survival rate improves significantly, ranging from 80% to 90%. Detecting it early and taking timely action is crucial, as oral cancer can spread to distant areas, making effective treatment more challenging (Deshmukh et al., 2021). It is essential to be aware of the severity of oral cancer and its potential consequences. Regular screenings, particularly for high-risk individuals, along with maintaining good oral health habits, can play a crucial role in detecting oral cancer at an early stage, improving the chances of successful treatment and better outcomes (Abat et al., 2020; Khanaga et al., 2021; Ketabat et al., 2019).

In recent years, advancements in machine learning algorithms have shown promising results in various medical applications, including cancer detection. These algorithms have played a significant role in predicting OSCC biopsies, offering improved accuracy in classification and aiding in prognosis. (Rahman et al., 2022; Das et al., 2020; Rao et al., 2022). By leveraging data from diverse sources, such as patient medical records, imaging, and genetic profiles, machine-learning models can assist clinicians in making more informed decisions, leading to better patient outcomes (Kirubabai et al., 2021; Bansal et al 2022; Huang et al., 2022). Also explores the importance of early oral cancer detection, the prevalence and characteristics of oral squamous cell carcinoma, and the growing role of machine learning algorithms in predicting OSCC biopsies. Bur et al., (2019). A comprehensive analysis of these factors, highlights the potential benefits of integrating machine learning techniques into oral cancer diagnosis and management, ultimately contributing to enhanced patient care and survival rates. Warin et al., (2021). Oral cancer affects various areas in the mouth and presents symptoms such as non-healing sores, lumps, difficulty chewing or speaking, and swollen jaw. Tobacco usage, alcohol intake, and HPV infection are all risk factors. The tumor stage is determined by the location, size, and involvement of lymph nodes (Chamoli et al., 2021; Capote-Moreno et al., 2020).

Machine learning is an artificial intelligence technique that enables computer systems to learn from data without requiring explicit programming. It can be categorized into supervised and unsupervised learning (Panigrahi et al., 2022; Janiesch et al., 2021). In supervised learning, labelled data is used to make predictions, while unsupervised learning aims to identify patterns in unlabelled data. El-Hasnony et al., (2022). Classical machine learning models like Support Vector Machine (SVM) and Decision Tree (DT) are applied for the classification of oral cancer, aiding in diagnostic and predictive tasks. (Dixit et al., 2023; Parkavi et al., 2023). In cases where existing classification algorithms fail to produce satisfactory results, the development of novel approaches becomes necessary. The primary contributions of this paper can be summarized as follows,

- Data collection, involving the gathering of real-time information from Arthi Scan Hospital, plays a pivotal role in enhancing the practical relevance of the system for oral cancer detection.
- Utilizing the Bee Pulse Couple Neural Network (BeePCNN) method for segmentation demonstrates a novel and innovative approach to image analysis.
- Incorporating FGPSOCNN for oral cancer detection underscores the application of a specialized and effective classification technique within the context of this critical medical concern.

The paper is structured as follows, Section 2 discusses relevant contemporary literature, Section 3 provides a detailed description of the proposed architecture, Section 4 presents the experimental results and subsequent discussions, and Section 5 concludes the paper, offering insights into future research directions.

## 2. Literature Review

Bhandari et al., (2020) proposed a CNN architecture with a tailored loss function designed to minimize errors, reduce overfitting, and support multi-class classification. The derivation of the modified loss function involves a combination of the Mean Squared Error (MSE) rate with the cross-entropy loss function. The strategic use of the ReLU activation function within the convolutional layer augments the model's training capabilities, simultaneously mitigating the risk of data overfitting. However, it is essential to acknowledge the potential complexity introduced by the customized loss function, which may require careful parameter tuning and could prolong the training process, making it resource-intensive. Das et al., (2018) focused on automating the identification of clinically significant regions within histological images of oral tissue, particularly for the diagnosis of oral squamous cell carcinoma. Folmsbee et al., (2020) introduced active deep-learning techniques to enhance the training efficiency of convolutional neural networks for tissue classification in oral cavity cancer, demonstrating improvements in accuracy and performance. This approach made advancements in medical image analysis for cancer diagnosis.

In Xu et al., (2019), the authors proposed a 3DCNN-based algorithm for the early diagnosis of oral cancer. The algorithm was trained on a dataset of 3D CT images of oral cancer patients.

The authors also used data augmentation to increase the size of the training dataset. This helped to improve the performance of the algorithm. The authors concluded that their algorithm is a promising approach for the early diagnosis of oral cancer, even if those features are not present in all the training data. The authors implemented a transfer learning approach in Amin et al., (2021), fine-tuning three pre-trained deep learning models individually (VGG16, InceptionV3, and ResNet50) and subsequently combining them for feature extraction. This concatenated model outperformed individual models, achieving high accuracy. In Musulin et al., (2021), the power of CNNs in tandem with a conditional random field model to achieve precise grading of oral OSCC and the segmentation of epithelial and stromal tissue. Their model was trained on an extensive dataset of histopathological images, annotated for both OSCC grading and tissue segmentation. Alhazmi et al., (2021) delved into the realm of AI and machine learning, aiming to predict the risk of oral cancer. Their work involved employing advanced computational models to assess an individual's vulnerability to this type of cancer, potentially enabling proactive preventive measures. Conversely, Chu et al., (2020) directed their attention toward the prognosis of treatment outcomes in oral cancer. Utilizing AI, their study sought to equip healthcare professionals with valuable insights into patients' likely responses to different treatment approaches, facilitating personalized therapeutic decision-making.

Additionally, Welikala et al., (2020) introduced an automated deep learning-based system for detecting and classifying oral lesions. While these approaches hold promise, it's important to note that they come with high computational complexity, which may present practical challenges in real-world clinical applications. Myriam et al., (2023) introduced an innovative meta-heuristic algorithm for oral cancer detection, combining particle swarm optimization (PSO) and Al-Biruni earth radius optimization (BER) methods. This hybrid approach effectively initializes a deep belief network (DBN) with PSO and fine-tunes it using BER, achieving efficacy accuracy on a challenging dataset. However, the paper could benefit from a more extensive discussion of potential limitations, such as computational resource requirements, scalability, and robustness across diverse datasets. In Arijji et al., (2020) presented an approach using the Alexnet architecture for oral cancer detection from MRI images, achieving a notable 84.7% accuracy on a test set from oral cancer patients. The utilization of the DIGITS deep learning training system led to the creation of five learning models after 300 epochs. However, it is crucial to acknowledge the observed lower accuracy as a significant point of consideration. Jubiar et al., (2022) introduced the Light-Weight Deep Convolutional Neural Network (LWDCNN) for oral cancer image analysis, featuring efficiency and speed without compromising accuracy through transfer learning. Deif et al., (2022) employed a hybrid feature selection approach, combining statistical analysis, correlation coefficients, and a genetic algorithm to enhance the classification of colorectal cancer histology using SVM. Ghosh et al., (2022) developed a novel Deep-Reinforced Neural Network (DRNN) for oral cancer risk prediction, leveraging deep and reinforcement learning, and integrating cell images and cyto-spectroscopic data for improved predictive accuracy.

Patibandla, S.K. et al., (2023) designed an oral cancer detection model using CNN. This method integrates an edge-based segmentation technique with labelled pixel extraction. While the approach holds the potential to improve image quality and enhance cancer detection accuracy, its complexity due to the combination of these techniques leads to longer processing times and increased resource demands, requiring careful optimization to strike a balance between accuracy and computational efficiency. In Wahid et al., (2022), the study introduces an automated approach for segmenting oropharyngeal cancer tumor volumes using MRI scan images. The Residual U-net, a deep learning architecture, is employed to facilitate this segmentation process, while the Dice similarity coefficient serves as the key metric for evaluating the model's performance. The advantages of such automated segmentation include increased efficiency and reduced inter-observer variability. However, it is important to note potential drawbacks, such as the model's reliance on large and diverse datasets for training and the challenge of interpreting the decisions made by complex deep learning models, which may lack transparency and require careful validation.

Building upon the insights from the literature analysis, the current study delves into the classification of oral MRI images. The study introduces novel variations and layers within the FGPSOCNN architecture.

### 3. Research Methods

The oral cancer detection process commences by collecting input MRI images, which then undergo a crucial pre-processing stage utilizing an Adaptive Bilateral Filter (ABF). This filter is a type of image enhancement technique that helps to reduce noise and preserve important structural details in the image, making it particularly useful for medical imaging. After pre-processing, pattern-based features such as Local Optimal Orientated Pattern (LOOP) and LTP are extracted. After that, the patterns are subjected to a segmentation process. The Bee Pulse Couple Neural Network (BeePCNN) segmentation method is employed to separate the cancer-affected regions, which can help in isolating specific structures of interest within the image. The BeePCNN is a neural network-based approach that is designed to identify and delineate regions within images. Following the segmentation step, the segmented regions are then subjected to a classification process using the proposed FGPSOCNN method. This classification step is where the system determines whether the segmented regions are normal or abnormal. FGPSOCNN is a specialized type of CNN that considers not only the spatial organization of features in the image but also incorporates fuzzy logic principles and hyperparameters tuned by genetic PSO for handling uncertainties in the classification process. By combining these techniques, the system aims to achieve accurate identification of abnormal regions in the CT image, which is crucial for detecting potential health issues. This comprehensive approach depicted in Figure 1, involving pre-processing, segmentation, and classification, helps enhance the accuracy and reliability of the analysis, contributing to more effective medical imaging evaluation and diagnosis.

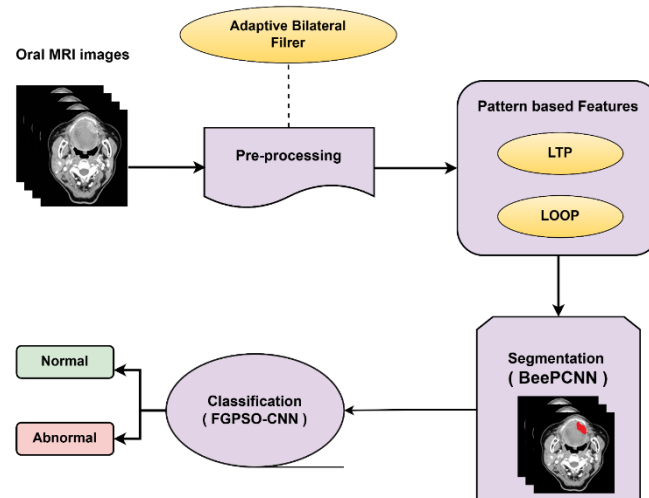


Fig. 1. The Overall Design of The Proposed Oral Detection Model

#### 3.1. Dataset

The oral cancer detection process begins with the acquisition of real-time MRI images from the Arthi Scan Hospital. MRI images obtained using a 3.0 Tesla MRI machine are known for their high image quality due to the stronger magnetic field. Storing these images in DICOM format (.dcm) is a standard practice in the medical field, as it allows for comprehensive information about the image and the patient to be stored together. This dataset consisting of a total of 1036 samples that encompass cases involving the presence of oral cancer and normal case.

#### 3.2. Pre-processing

Pre-processing enhances MRI image quality by reducing noise using Adaptive Bilateral Filter (ABF). The ABF is a sophisticated technique used in MRI image pre-processing. ABF not only reduces noise but also preserves edges and fine details by considering local image characteristics.

For an input image  $I(a, b)$  and a pixel location  $(a, b)$  within the image, the filtered output  $F_{out}(a, b)$  within the defined neighbourhood pixel  $\varphi$ , using the ABF can be expressed as,

$$F_{out}(a, b) = \frac{1}{\mu} \sum_{b \in \varphi} W_s(|a - b|) W_r(|I_a - I_b|) I_a$$

Where,  $W_s(|a - b|)$  is the spatial weight, dependent on the spatial distance between the central pixel  $a$  and the neighboring pixel  $b$ ,  $W_r(|I_a - I_b|)$  is the range weight, determined by the absolute difference between the intensity values of the central pixel  $I_a$  and the neighboring pixel  $I_b$ , and  $\mu$  is the normalization factor defined below,

$$\mu = \sum_{b \in \varphi} W_s(|a - b|) W_r(|I_a - I_b|)$$

Upon the completion of the pre-processing stage, the subsequent step in the pipeline involves feature extraction.

### 3.3. Feature Extraction

Feature extraction involves identifying and capturing meaningful information from the pre-processed images that can be used to distinguish between different classes or categories, such as oral cancer and normal cases.

#### 3.3.1. Local Optimal Orientated Pattern (LOOP)

The LOOP is combines the strengths of Local Directional Pattern (LDP) and Local Binary Pattern (LBP) while overcoming their respective issues. LBP is a well-known descriptor that captures local intensity variation patterns in an image and demonstrates good discrimination characteristics. On the other hand, LDP is an improved local pattern descriptor that incorporates a directional component using Kirsch compass kernels, making it less susceptible to noise compared to traditional LBP. However, both LDP and LBP suffer from a major issue: the randomized sequence of binarization weights, which introduces dependency on orientation. To address this problem, the LOOP method incorporates additional information by assigning binarization weights to neighboring pixels based on the strength of Kirsch output in the direction of each pixel. The enhanced LDP descriptor in LOOP effectively introduces a directional component with Kirsch compass kernels, making it less vulnerable to noise compared to the original LBP operator. This adaptability and scale-independence make it a potential candidate for improving oral cancer detection algorithms. The LOOP feature for the pixel  $(r_1, r_2)$  is defines as,

$$F_{loop}(r_1, r_2) = \sum_{v=0}^{A-1} k(z_v - z_0) * 2^{w_v}$$

Where  $z_0$  is the pixel intensity of an image at  $(r_1, r_2)$ , an exponential value, denoted as  $w_v$ , is assigned to each of these neighboring pixels, taking a digit between 0 and A-1, and  $z_v$  represents the Kirsch masks are oriented in the direction of the neighboring pixel intensity ( $v = 1, 2, \dots, A - 1$ ), providing a measure of the intensity variation strength.

$$z(r) = \begin{cases} 1, & \text{if } x \geq 0 \\ 0, & \text{if } x < 0 \end{cases}$$

The main formulation of the LOOP descriptor encodes rotation invariance, allowing it to handle varying orientations in an image.

#### 3.3.2. Local Ternary Pattern (LTP)

LTP is an extension of the LBP operator and the basic idea of LTP is to compare the central pixel value with its neighbors in a circular region around it by thresholding, and then encode the comparisons into a ternary code. The LTP operator is formed by combining the coded

representations of two distinct patterns: the upper pattern and the lower pattern. LTP is designed to capture texture information and helps to detect the oral cancer-affected region. The LTP operator can be represented with the following equation:

$$F_{ltp}(r_1, r_2) = \sum_{v=0}^{A-1} k(z_v - z_0) * 3^v$$

$$z(r) = \begin{cases} 1, & r \geq \alpha \\ 0, & \alpha < r < \alpha \\ -1, & r < -\alpha \end{cases}$$

Where,  $\alpha$  denotes threshold value, and  $3^v$  represents the weight to emphasize the importance of certain positions within the neighborhood.

### 3.4. Segmentation

Upon obtaining pattern images, the following stage involves segmentation, wherein the goal is to precisely delineate cancer-affected areas by outlining their boundaries within the images. This accurate boundary identification holds significance for effective cancer diagnosis.

#### 3.4.1. Bee Pulse-Coupled Neural Network (BeePCNN)

The BeePCNN segmentation method employs a Pulse-Coupled Neural Network (PCNN) framework, with hyperparameters fine-tuned using the Artificial Bee Colony (ABC) algorithm, to enhance the accuracy and effectiveness of the segmentation. Optimization problems are common across diverse domains, but classical methods face efficiency issues, especially with high dimensions. Heuristic approaches, such as the ABC algorithm, offer a powerful alternative. ABC, inspired by the social interactions of honeybees, has proven successful, particularly in handling NP-hard problems and searching for optimal hyperparameters in machine learning algorithms. This study focuses on leveraging ABC to significantly reduce tuning time for models. Hyperparameters tuning is carried out using the ABC algorithm is a promising approach to find optimal configurations for PCNN. The ABC algorithm's ability to handle complex optimization problems makes it well-suited for the high-dimensional search space of hyperparameters. The BeePCNN architecture is shown in Figure 2.

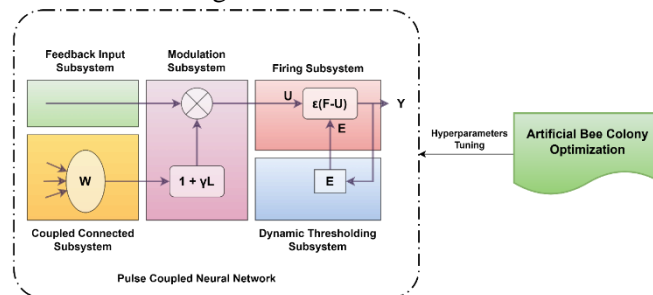


Fig. 2. Architecture of BeePCNN

**PCNN:** The PCNN model originates from a configuration of pulse-coupled neurons arranged in a two-dimensional array. This model, often used for image segmentation, represents pixels as neurons within this array. When a neuron in the PCNN model undergoes firing, it triggers the simultaneous firing of all pixels within the same category. This phenomenon arises from the inherent neuron coupling present in the model. Leveraging this coupling behaviour, the PCNN model employs various techniques to process digital images. This approach capitalizes on the synchronized activation of pixels to accomplish image analysis tasks. By harnessing the interconnected nature of the neurons, the PCNN model demonstrates its effectiveness in dealing with digital imagery. The PCNN model comprises distinct subsystems with corresponding equations. The coupled connection subsystem is defined as,

$$\Phi_{xy}(l) = K_{xy}$$

Where,  $\Phi_{xy}(l)$  and  $K_{xy}$  are denote the feedback input and external input excitation respectively. The input feeding subsystem, modulation, and dynamic threshold subsystems are expressed as,

$$X_{xy}(l) = \sum_{i,j} \Phi_{xy,ij}(l) H_{ij}(l - 1)$$

$$Y_{xy}(l) = \Phi_{xy}(l) (\delta * X_{xy}(l) + 1)$$

$$H_{xy}(l) = \begin{cases} 1, & Y_{xy}(l) > M_{xy}(l - 1) \\ 0, & otherwise \end{cases}$$

Where,  $X_{xy}(l)$  represents connect input for the model,  $Y_{xy}(l)$  is internal activity term within the neural network, and  $H_{xy}(l)$  is pulse output value of the neural network,  $\Phi_{xy,ij}$  is connection weight matrix between neurons. Dynamic threshold  $\theta_{xy}(l)$  within the neural network is defined as,

$$\theta_{xy}(l) = e^{-\alpha_M} * M_{xy}(l - 1) + V_M * H_{xy}(l)$$

Where,  $\delta$  is connection coefficient,  $\alpha$  and  $V_M$  are the amplitude constants and time decay constants of the dynamic threshold, respectively.

Image segmentation focuses on neuron-triggered firing, either naturally or via neighbours. Neurons fire once per iteration, ensuring minimum threshold attenuation to enable firing chances. All neurons can fire when dynamic threshold reaches minimal attenuation. Neighbouring neuron firing estimates adjacent pixel gray levels, reflecting pixel value changes. Prior knowledge of neuron firing aids estimating defocused image region characteristics. PCNN neurons trigger neighbours through connection and feedback. In successive iterations, dynamic threshold decay leads to adjacent neuron firing. This process helps refine regional estimations in defocused images. The PCNN model interplay of subsystems and firing dynamics facilitate effective image analysis and segmentation.

**PCNN hyperparameter tuning using ABC:** Initially, hyperparameters space is defined, this includes the range of values for each hyperparameters in PCNN. The search space for hyperparameters tuning involves the learning rate, momentum, hidden neurons, batch size, and epochs. After that initial solutions can be randomly generated within the defined hyperparameters search space. Generate a random population  $Q_{i,j}$  for a variable space specified lower  $LB_j$  and upper  $UB_j$  bounds by adding a random offset between 0 and 1 times the range of the bounds.

$$Q_{i,j} = LB_j + rand(0,1) * (UB_j - LB_j)$$

Next, Evaluate the fitness of each solution using the objective function in equation (13). This step determines how well each set of hyperparameters performs on the given task. In this study, the selected fitness function is the mean square error (MSE) of the model when evaluated on the training set. This can be represented as,

$$Fit = \frac{1}{n} \sum_{i=1}^n (y_i - \hat{y}_i)^2$$

Where,  $n$  is the number of samples,  $y_i$  represents the actual (observed) value for the  $i^{th}$  sample, and  $\hat{y}_i$  represents the predicted value by the model for the  $i^{th}$  sample. The employed bees update their solutions by making small perturbations to the existing hyperparameters. The updated solutions  $V_{i,j}$  are evaluated for fitness is defined as,

$$V_{i,j} = \begin{cases} Q_{i,j} + \zeta * (Q_{i,j} - Q_{k,j}), & rand < M_r \\ Q_{i,j}, & otherwise \end{cases}$$

Here,  $M_r$  is the modification rate. Onlooker bees select solutions based on their fitness, with better solutions having a higher probability of being chosen. These onlooker bees generate new solutions similarly to the employed bees. If a solution has not improved for a predefined number of iterations, it becomes a scout bee. The scout bee abandons its current solution and explores a new random solution within the search space. If a new solution found by an onlooker bee has better fitness than the solution it replaces in the population, the population is updated. The algorithm continues for a certain number of iterations or until a convergence criterion is met. By iteratively updating the population of solutions, ABC explores the hyperparameters search space, focusing regions and gradually converging toward optimal hyperparameters settings.

### 3.5. Classification

In this process, a segmented image of the oral cavity is analyzed using a classification model to determine whether it exhibits normal or abnormal characteristics related to oral cancer. These segmented images are then input into a trained classification model that has learned patterns from labelled data. The model output prediction helps identify potential abnormalities, aiding in early detection and decision-making for further medical evaluation if necessary.

#### 3.5.1. Proposed FGPSOCNN based classification

The proposed classification approach involves utilizing a novel technique called FGPSOCNN, which likely stands for Fuzzy Genetic Particle Swarm Optimization Convolutional Neural Network. This hybrid methodology integrates the CNN, with fuzzy logic for improved performance in classification tasks. Fuzzy logic is used to handle uncertainty and imprecision in data. By incorporating fuzzy logic, the proposed method might be more robust to variations and uncertainties in the data, leading to better classification results. Also, hyperparameters are tuned by Genetic PSO algorithm. PSO is an optimization algorithm inspired by the collective behavior of swarms in nature. In the context of classification, PSO likely optimizes specific parameters or features to enhance the effectiveness of the subsequent classification process. Genetic Algorithms explore a broad solution space, aiming to find the global optimum rather than getting stuck in local optima. This characteristic is crucial for ensuring the classification model's parameters are finely tuned across various scenarios. PSO iteratively refines solutions within a search space to find optimal values. This hybrid approach showcases a multidisciplinary approach to address classification challenges in a more sophisticated manner. The schematic representation of the proposed FGPSOCNN model is depicted in Figure 3.

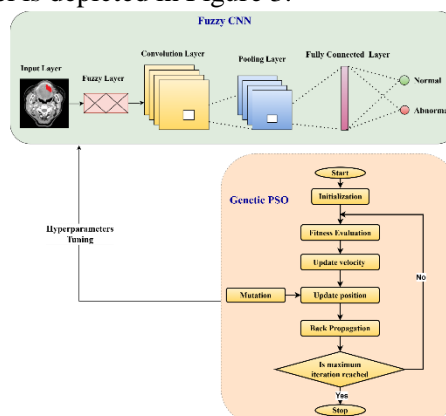


Fig. 3. The proposed FGPSOCNN model

#### 3.5.2. Fuzzy Convolutional Neural Network (Fuzzy CNN)

CNN have achieved impressive results in image classification tasks. However, when dealing with medical images, uncertainties and imprecisions arising from factors like varying lighting conditions, tissue appearance, and image quality can undermine classification accuracy.

To overcome these challenges, the incorporation of fuzzy logic into CNNs emerges as a viable solution. This integration allows for the effective management of uncertainties in the decision-making process, offering a means to mitigate the impact of diverse uncertainties encountered in medical image analysis.

**Input Layer**

The input layer of the Fuzzy CNN receives segmented oral images and passes their pixel values to the network. It acts as a starting point, conveying the image information for further classification. The input layer of the Fuzzy CNN can be represented as:

$$I = [Se_1, Se_2, \dots, Se_i, \dots, Se_n], \quad (N = 1, 2, 3, \dots, n)$$

Where  $N$  denotes the total number of images,  $I$  the input vector containing pixel values of the segmented oral image, and  $Se_i$  represents the  $i^{th}$  pixel value.

**Fuzzy layer**

When an image is input into the fuzzy layer, each pixel value is considered as an input value. These input values are then transformed using the predefined fuzzy membership functions

Each pixel value is mapped to membership degrees across different categories based on these functions. The working of fuzzy layer is explained as follows.

*Fuzzy Membership Functions:* Texture-based membership functions play a significant role in oral cancer detection using CNN. These functions are tailored to capture the texture characteristics of oral images, aiding in accurately classifying healthy and cancerous tissues. The texture-based membership functions based on Gaussian distributions with uncertain mean, uncertain standard deviation, and both uncertain mean and uncertain standard deviation can be defined as,

$$\mu_{ij}(x; u', \sigma) = \alpha_j \frac{1}{\sqrt{2\pi}\sigma_j} \exp\left\{-\frac{(x_i - u_j)^2}{2\sigma_j^2}\right\}, \quad u_j \in [u_j^-, u_j^+]$$

$$\mu_{ij}(x; u, \sigma') = \alpha_j \frac{1}{\sqrt{2\pi}\sigma_j} \exp\left\{-\frac{(x_i - u_j)^2}{2\sigma_j^2}\right\}, \quad \sigma_j \in [\sigma_j^-, \sigma_j^+]$$

$$\mu_{ij}(x; u', \sigma') = \alpha_j \frac{1}{\sqrt{2\pi}\sigma_j} \exp\left\{-\frac{(x_i - u_j)^2}{2\sigma_j^2}\right\}, \quad u_j \in [u_j^-, u_j^+], \sigma_j \in [\sigma_j^-, \sigma_j^+]$$

Where,  $u'$  and  $\sigma'$  denote mean and standard deviation of healthy tissue pixel.  $u_j^-, u_j^+$  and  $\sigma_j^-, \sigma_j^+$  are the left and the right pixel of the healthy pixel mean and standard deviation. These membership functions are specifically tailored to each tissue class, capturing their distinct textural attributes. The upper and lower membership functions of the interval type-2 fuzzy model for each class can be mathematically expressed as follows,

$$\mu_{ij}^+(x) = \begin{cases} \mu_{ij}(x; u^-, \sigma) , & x_i < u_j^- \\ \alpha_j & , u_j^- < x_i < u_j^+ \\ \mu_{ij}(x; u^+, \sigma) , & x_i > u_j^+ \end{cases}$$

$$\mu_{ij}^-(x) = \begin{cases} \mu_{ij}(x; u^-, \sigma) , & x_i \leq \frac{u_j^- + u_j^+}{2} \\ \mu_{ij}(x; u^+, \sigma) , & x_i > \frac{u_j^- + u_j^+}{2} \end{cases}$$

These Gaussian distribution formulations with uncertain mean, uncertain standard deviation, and both uncertain mean and uncertain standard deviation enable the modeling of uncertain and varying texture characteristics present in oral images, thus contributing to more robust and accurate oral cancer detection using a Fuzzy CNN approach. By integrating these texture-based membership functions into the network operations, the model becomes capable of handling the uncertainty inherent in oral image texture attributes. This enhanced capability enables the network to discern subtle textural differences between healthy and cancerous tissues

*Fuzzification Process:* The fuzzification process assigns membership degrees to each pixel value based on the membership functions. This process is essentially a mapping of pixel values to membership degrees in different fuzzy sets. The membership degrees represent how much a pixel value belongs to a specific attribute category.

*Fuzzy Pixel Representation:* After the fuzzification process, each pixel in the image is represented not by a single value but by a set of membership degrees corresponding to various fuzzy sets. This representation captures the uncertainty and vagueness associated with pixel attributes.

**Convolution layer**

The fuzzy pixel representation is then integrated into the convolutional layers. The convolutional layers apply convolution operations to the fuzzy pixel values, considering the membership degrees along with the convolutional filters. The convolutional layers function as feature extractors, responsible for learning feature representations from the corresponding input images. Within the convolutional layers, neurons are organized into feature maps, each containing a receptive field. These neurons are interconnected with the neighbourhoods of neurons in the preceding layer via a set of trainable weights referred to as the filter bank. Through the process of convolving the inputs with the learned weights, a novel feature map is generated. The convolved results then traverse the neurons within the feature map, each equipped with nonlinear activation functions and associated weights. These neurons maintain consistent weight conditions. Within the same convolutional layer, multiple feature maps are established, each composed of distinct weights for extraction at various locations. In general, the calculation of the  $v^{th}$  output feature map  $R_v$  is carried out as presented below,

$$R_v = \mathcal{F}(C_{f_v} * P_{in})$$

In this context, the non-linear activation function is represented by  $\mathcal{F}(\cdot)$ , while the two-dimensional convolutional operation is indicated by the multiplication sign,  $C_{f_v}$  signifies the convolutional filter associated with the  $v^{th}$  feature map, and  $F$  denotes the input image after undergoing fuzzy layer.

**Pooling layer**

Pooling layers in the fuzzy CNN down sample fuzzy pixel representations while retaining the membership degrees. This down sampling aids in reducing spatial resolution within the feature maps, contributing to spatial invariance against translations and distortions in the input. Through pooling aggregation, average values are computed across the input area, and the resulting output maps are formed by convolving multiple input maps, as specified by Eq. (2).

$$R_k^a = \mathcal{F}\left(\sum_{l, I_m} R_k^{a-1} * \Psi_{l,k}^a + Ab_k^a\right)$$

The equation presented above signifies the selection of input maps denoted by  $I_m$ , where  $a$  corresponds to the convolutional layer with the  $l^{th}$  input and  $k^{th}$  output. The additive bias of the convolutional layer  $a$  is represented as  $Ab^a$ , and the kernel maps of this layer are denoted as  $\Psi_{l,k}$ . The preceding down sampling layer is referred to as  $a - 1$ , and its input features are represented by  $R^a$ .

### **Fully Connected layer**

Numerous abstract feature representations are derived by amalgamating the diverse pooling and convolutional layers. These representations encapsulate essential characteristics, which are subsequently deciphered by the fully connected layers to perform sophisticated high-level reasoning operations.

### **Output layer**

The output layer is responsible for providing the final classification result. For the classification scenario of healthy tissue and cancerous tissue, there would be two neurons in the output layer. The values produced by these neurons are often transformed using an activation function, such as the softmax function, to convert them into probabilities representing the likelihood of the input image belonging to each class.

### **3.2.4 Training**

The tuning of hyper parameters is achieved through the utilization of learning algorithms to acquire the desired network output. The commonly employed algorithm for this purpose is back propagation. To enhance the effectiveness of the current Fuzzy CNN architecture, optimization of the activation function, hidden neurons, and batch size is accomplished by employing the proposed Genetic PSO technique. This approach aims to achieve the highest accuracy level possible.

### **3.5.3. Genetic Particle Swarm Optimization (Genetic PSO)**

Prior research has primarily focused on addressing individual challenges within optimization, such as the intricacies of hyperparameters tuning or the complications posed by local minimums. The novel approach aims to enhance Fuzzy CNN performance by concurrently addressing both aspects. In this model, the power of Genetic Algorithms (GA) and Particle Swarm Optimization (PSO), in conjunction with the Backpropagation (BP) algorithm, to cohesively optimize both the network hyperparameters and connection weights. The algorithm for the proposed FGPSOGAN is defined as,

*Initialization:* Initialize the genetic parameters and particle swarm weight factors. Based on the coding scheme, the hyperparameters binary coding to be considered to decide the kernel size, batch size, learning rate, and the number of filters. In contrast, connection weights will employ real number coding. A direct correspondence is established between the connection weights of individual network nodes. Begin by randomly generating  $M$  initial solutions.

*Fitness Evaluation:* The evaluation of the fitness function is pivotal for identifying the optimal hyperparameters. Fitness values are computed using equation (7), a comparison reveals the solution with the best fitness.

*Position update:* Update the present optimal solution and the individual optimal solution as  $P_g = [P_g^{(1)}, P_g^{(2)}]$ ,  $P_i = [P_i^{(1)}, P_i^{(2)}]$  respectively. Then update the global best fitness.

*Velocity and position update:* In the optimization process, the velocity of each particle in the swarm needs to be updated to guide its movement towards better solutions. This velocity update equation is defined as,

$$Ve_z(\tau + 1) = \omega * Ve_z(\tau) + c_1 * r_2 * (P_{best} - X_z) + c_2 * r_2 * (G_{best} - X_z)$$

Where,  $Ve_z(\tau + 1)$  is the updated velocity,  $Ve_z(\tau)$  is the current velocity,  $\omega$  is the inertia factor,  $c_1$  and  $c_2$  are learning factors,  $r_1$  and  $r_2$  are random values in the interval  $[0, 1]$ ,  $P_{best}$  is the individual optimal position reached by the particle,  $G_{best}$  is the global optimal position, and  $X_z$  is the current position of the particle.

The mutation operation in the GA is included during the binary position update of particles to introduce randomness and enhance exploration. This helps prevent being stuck in local optima

and boosts the chances of finding the global optimum by allowing particles to explore new areas in the solution space. The real and binary part of the particle's position is updated based on the principles outlined as,

$$M(Ve_z) = \frac{1}{1 + \exp(-Ve_z)}$$

$$X_z = \begin{cases} X_z, & rand < M(Ve_z) \\ 1 - X_z, & otherwise \end{cases}$$

$$E_h = \frac{L_h - U_h}{2 * N_{var}}$$

$$X_{z,\tau,j} = \begin{cases} X_{z,\tau,j} + d[-0.5,0.5]E_h, & X_{z,\tau,j} = G_j \text{ or } d \in [0, C_r] \\ G_j + d[-0.5,0.5]E_h, & X_{z,\tau,j} \neq G_j \text{ or } d \in [C_r, C_g] \\ X_{z,\tau,j} + d[-0.5,0.5](X_{z,\tau,j} - G_j), & X_{z,\tau,j} \neq G_j \text{ or } d \in [C_g, 1] \end{cases}$$

Where,  $M$  signifies the probability of changing the particle's position,  $X_{z,\tau,j}$  denotes the value of the  $j^{th}$  site of  $z^{th}$  particle in the  $\tau^{th}$  iteration,  $d$  is a randomly generated number in  $[0, 1]$ ,  $G_j$  signifies the value of the  $j^{th}$  site of the global optimal particle,  $C_r$  and  $C_g$  are constants given,  $E_h$  pertains to a speed parameter,  $L_h$  and  $U_h$  represent the upper and lower bounds of the variable, respectively,  $N_{var}$  stands for the number of variables.

*Back propagation:* Conduct  $n$  backpropagation (BP) iterations on particle  $z$ . After each iteration, update the value of the corresponding position in the real part of particle  $z$  based on the connection weight adjustments achieved during the iteration. The process continues as described above until it reaches the maximum iteration.

#### 4. Results and Discussions

This section presents the experimental analysis and comparative outcomes of the FGPSOCNN model proposed in this study. The model performance is thoroughly evaluated, and a comprehensive comparison is conducted with other pertinent methodologies. This assessment aims to gauge the effectiveness and capabilities of the proposed FGPSOCNN model.

##### 4.1 Experimental Setup

The proposed method for predicting oral cancer is implemented using MATLAB R2020a on a Windows 10 operating system equipped with 64-bit architecture and 32 GB of RAM. This setup offers a reliable and efficient environment to effectively execute the method with optimal performance.

##### 4.2 Data Description

The real-time MRI images was gathered from Aarthi Hospital. This compilation consists of 460 images that have been categorized as normal and an oral cancer affected 576 images categorized as abnormal. In order to facilitate analysis and processing, the original DICOM format of these images has been transformed into PNG format. Each individual image within this dataset has dimensions of 256 x 256 pixels and encompasses three color channels, resulting in a representation of 256 x 256 x 3 dimensions. A visual depiction of selected sample images from this dataset can be observed in Figure 4.

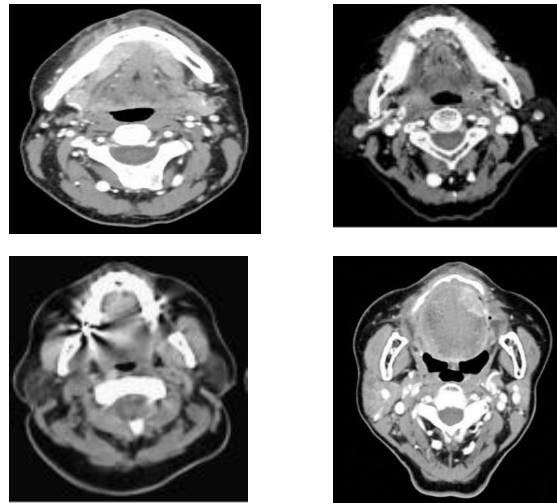


Fig. 4. Sample MRI oral scan images

In Figure 5(a), the showcased patterns highlight the unique characteristics and variations associated with the LOOP feature. Figure 5(b) presents the LTP feature, with displayed patterns that offer insights into its distinct characteristics and variations. These patterns provide visual insights into the qualities, aiding in understanding its structural attributes and potential functions.

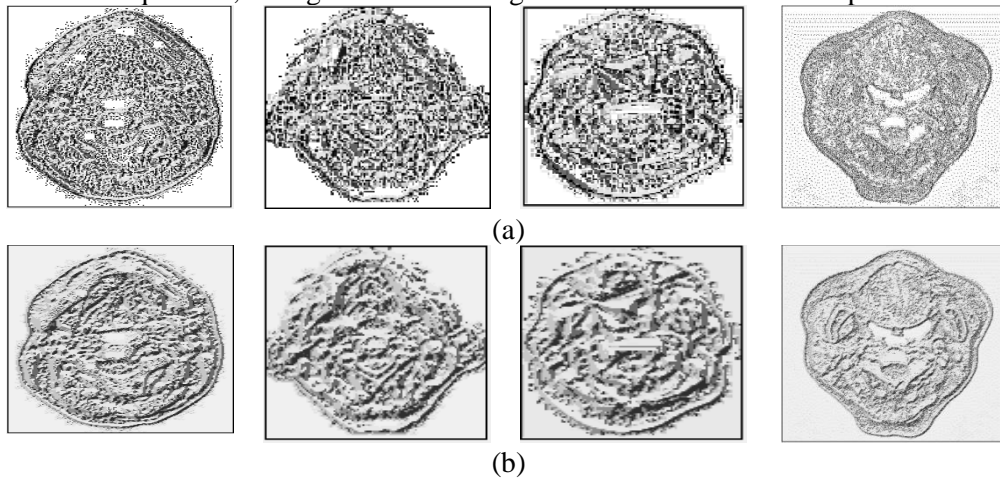


Fig. 5. Pattern features (a) LOOP (b)LTP

Figure 6 presents segmented images utilizing BeePCNN, effectively highlighting the detected regions linked to oral cancer. These segmented images distinctly emphasize the specific areas that have been identified as indicative of oral cancer, enabling a focused and precise visual representation of the affected regions.

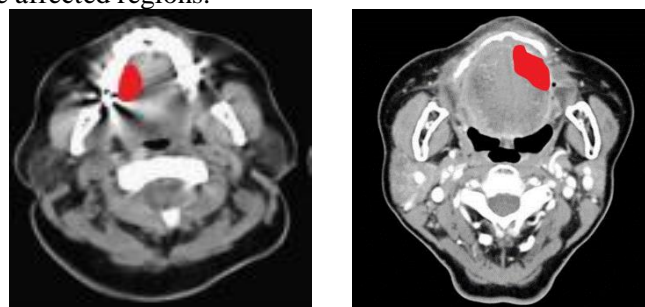


Fig. 6. Segmented images

### 4.3 Performance metrics

The assessment of the prediction algorithms in this study relies on various performance metrics are listed in Table 1.

Table 1 - Detection metrics

Metric	Formula	Explanation
--------	---------	-------------

Accuracy	$\frac{TP + TN}{TP + TN + FP + FN}$	Accuracy measures the ratio of correct predictions (both true positives and true negatives) to the total predictions, indicating overall model performance.
Precision	$\frac{TP}{TP + FP}$	Precision focuses on the proportion of true positive predictions compared to the total instances predicted as positive. It emphasizes prediction accuracy.
Recall	$\frac{TP}{TP + FN}$	Recall, also known as sensitivity or true positive rate, measures the proportion of actual positive instances correctly predicted as positive by the model.
F-score	$\frac{2 * (P * R)}{P + R}$	The F-score provides a balance between precision and recall, favouring models that achieve both high precision and recall, making it suitable for imbalanced datasets.
Error Rate	$\frac{FP + FN}{TP + TN + FP + FN}$	The error rate measures the ratio of incorrect predictions (both false positives and false negatives) to the total predictions, indicating overall prediction inaccuracy.
Specificity	$\frac{TN}{TN + FP}$	Specificity, also known as true negative rate, measures the proportion of actual negative instances correctly predicted as negative by the model.

In Table 1, P and R represents precision and recall, TP (True Positives) is the instances correctly predicted as positive by the model, TN (True Negatives) is the instances correctly predicted as negative by the model, FP (False Positives) denote the instances incorrectly predicted as positive by the model when they are negative, and FN (False Negatives) denote the instances incorrectly predicted as negative by the model when they are positive.

#### 4.4 Loss and Accuracy Curve

Figure 7 displays the accuracy curve of the proposed model, depicting its performance across the training and testing phases. Notably, the training phase employs 80% of the total samples, while the testing phase utilizes the remaining 20% for evaluation. The graph distinctly highlights the model efficacy, achieving an impressive accuracy rate of 97.22%, which serves as a testament to its strong performance. In Figure 8, the loss curve of the proposed model is displayed. This curve indicates that the model consistently achieved its optimal validation loss, ranging from 0.02 to 0.1, throughout both the training and testing stages. Notably, the model underwent 100 epochs as part of the accuracy and loss validation process. For a comprehensive overview of the hyperparameters employed in this study is listed in Table 2.

Table 2 - Hyperparameters Used For Classification

Parameters	Values
Loss function	Mean_squared_error
Optimizer function	adam
Metrics	accuracy
Epochs	100
Batch size	32
Learning rate	0.0001

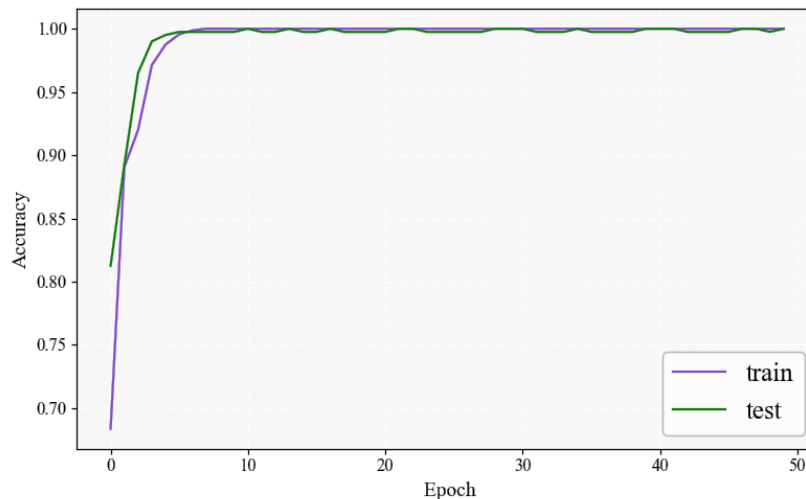


Fig. 7. Accuracy Curve For The Proposed Model

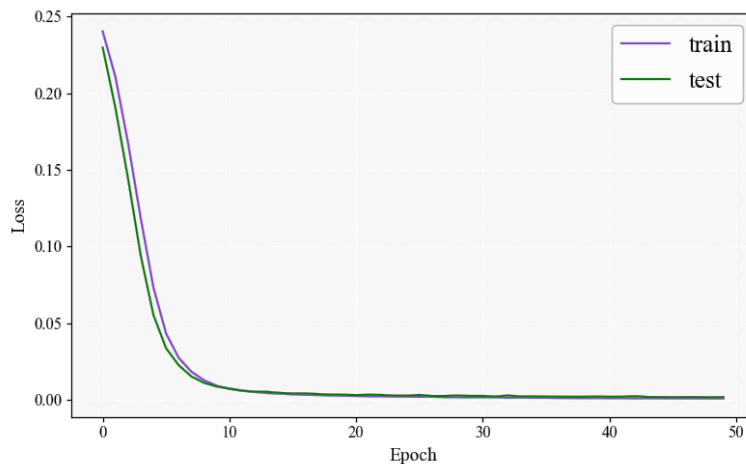


Fig. 8. Loss Curve For The Proposed Model

### 4.5 Comparative Analysis

In this section, a comparative analysis of the proposed FGPSOCNN model is undertaken to enhance the efficiency of oral cancer detection. The analysis considers several methods for comparison, including CNN Bur et al., (2019), 3D-CNN Warin et al., (2021), PSO-DBN Chamoli et al., (2021), Alexnet Capote-Moreno et al., (2020) and Residual U-Net Parkavi et al., (2023). The objective is to evaluate the effectiveness of the FGPSOCNN model in achieving accurate and efficient oral cancer detection, as compared to these existing methods.

The performance evaluation of the proposed FGPSOCNN model is conducted meticulously, and a comprehensive comparison is made against conventional methodologies, including CNN, 3D-CNN, PSO-DBN, Alexnet and Residual U-Net. The evaluation primarily employs the accuracy metric and is performed using 70% of the dataset for training and 30% for testing. The conventional methods yield moderate accuracy results, with values of 79.74%, 93.25%, 91.96%, 86.17%, and 93.12% achieved for CNN, 3D-CNN, PSO-DBN, Alexnet, and Residual U-Net, respectively. In contrast, the proposed method demonstrates a significant improvement, achieving an accuracy of 96.46%, which is superior by 3.44% in comparison to the existing techniques. For a more comprehensive and detailed understanding of the performance metrics, an in-depth analysis is available in Table 3.

Table 3 - Comparative Analysis Based On 70% Training And 30% Testing Data

Methods	Accuracy (%)	Precision (%)	Recall (%)	Specificity (%)	F1-Score (%)
CNN					
Bhandari et al., (2020)	79.74	77.54	76.98	81.98	77.26
3D-CNN					
Xu et al., (2019)	93.25	93.48	91.49	94.71	92.47
PSO-DBN					
Myriam et al., (2023)	91.96	91.30	90.65	93.02	90.97
Alexnet					
Ariji et al., (2020)	86.17	84.78	84.17	87.79	84.48
Residual U-Net Wahid et al., (2022)	93.01	93.27	89.97	94.38	91.68
Proposed FGPSOCNN model	96.46	96.38	95.68	97.09	96.03

The evaluation of the proposed FGPSOCNN model's performance has been meticulously carried out, and a thorough comparison has been conducted against established methodologies, including CNN, 3D-CNN, PSO-DBN, Alexnet and Residual U-Net. The assessment is primarily centered around the accuracy metric and has been executed by utilizing 80% of the dataset for training and 20% for testing. The conventional methods have produced accuracy outcomes of moderate nature, with respective values of 84.06%, 94.69%, 92.75%, 87.98%, and 94.20% achieved for CNN, 3D-CNN, PSO-DBN, Alexnet and Residual U-Net. In contrast, the proposed approach demonstrates a remarkable enhancement in performance, achieving an accuracy of

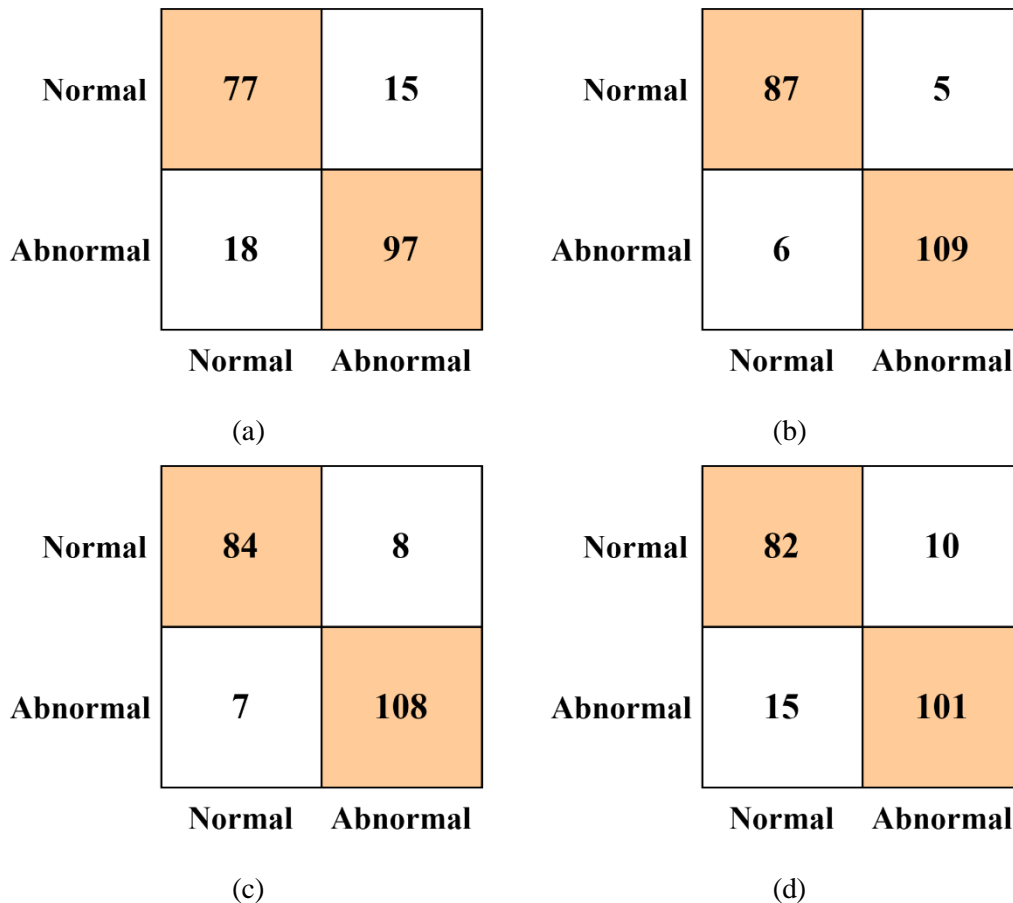
97.10%. This achievement stands superior by 2.5% when compared to the existing techniques. For an in-depth and comprehensive understanding of the performance metrics, an elaborated analysis has been provided in Table 4.

Table 4 - Comparative Analysis Based On 80% Training And 20% Testing Data

Methods	Accuracy (%)	Precision (%)	Recall (%)	Specificity (%)	F1-Score (%)
CNN					
Bhandari et al., (2020)	84.06	83.70	81.05	86.61	82.35
3D-CNN					
Xu et al., (2019)	94.69	94.57	93.55	95.61	94.05
PSO-DBN					
Myriam et al., (2023)	92.75	91.30	92.31	93.10	91.80
Alexnet					
Ariji et al., (2020)	87.98	89.13	84.54	90.99	86.77
Residual U-Net					
Wahid et al., (2022)	94.20	94.57	92.55	95.58	93.55
Proposed FGPSOCNN model	97.10	96.74	96.74	97.39	96.74

**4.2.1. Analysis of Confusion Matrix**

The effectiveness of the suggested classification approach is validated using a 2x2 confusion matrix for normal and abnormal nodules. The confusion matrices for various methods are shown in Figure9.



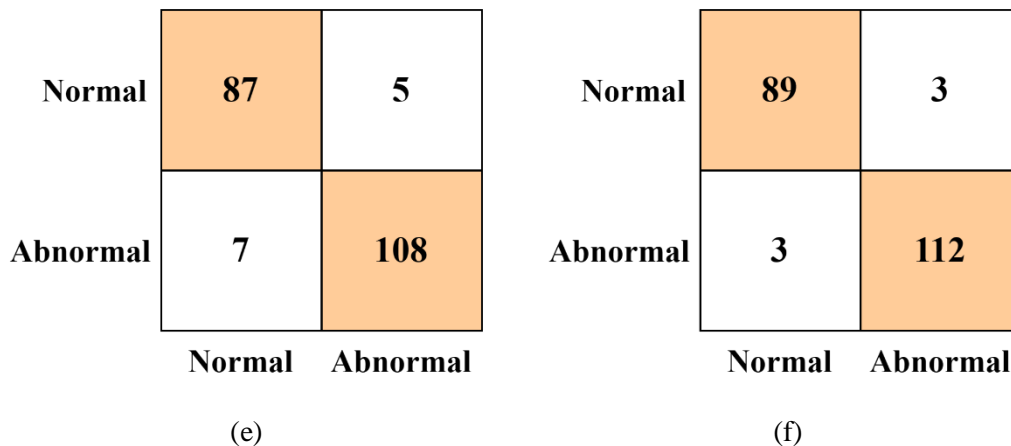


Fig. 9. The outcomes of confused matrices for various methods. (a) CNN, (b)3D-CNN, (c) PSO-DBN, (d)Alexnet, (e) Residual U-Net and (f)Proposed FGPSOCNN.

The analysis presented above underscores the impact of utilizing 80% of the training data within the proposed FGPSOCNN model, resulting in an exceptional performance boost for oral cancer prediction. This performance surpasses the accuracy levels achieved by conventional methods.

The proposed method demonstrates superiority over existing techniques in terms of various performance metrics. This superiority can be attributed to its adept utilization of preprocessing techniques that effectively enhance the quality of input data. Furthermore, the incorporation of BeePCNN segmentation proves instrumental in reducing computational time by precisely isolating the affected regions. As a result of these advancements, the oral cancer prediction achieved through the proposed FGPSOCNN model showcases a remarkable enhancement in prediction accuracy. This enhancement is primarily attributed to the integration of fuzzy logic into the CNN architecture, which empowers the model to extract intricate features and patterns from the data, thereby improving its predictive capabilities.

In essence, the proposed FGPSOCNN model offers an efficacy approach that optimizes multiple aspects of the prediction process. By synergistically leveraging preprocessing techniques, efficient region segmentation, and the fusion of fuzzy logic and CNN, the model achieves a substantial performance leap in the challenging task of oral cancer prediction

### 5. Conclusion

This study presents a focused exploration into the detection of oral cancer using real-time MRI images. The research introduces novel deep learning techniques for the accurate diagnosis of oral cancer. The proposed approach revolves around effective feature extraction and segmentation through the innovative BeePCNN technique. For classification, a novel method called FGPSOCNN is introduced, enhancing accuracy. The study leverages powerful feature extraction techniques, namely LOOP and LTP, to effectively capture meaningful patterns from the data. The dataset used for evaluation is derived from Arthi Scan Hospital, comprising real-time MRI images. Experimental results showcase the superiority of the novel FGPSOCNN model over existing methodologies. Through comparative analysis with conventional techniques, the proposed model remarkable performance comes to light. The model achieves impressive rates of accuracy (97.10%), precision (96.74%), recall (96.74%), specificity (97.39%), and f1-score (96.74%). Future research could explore improved tumor classification and model enhancement. Additionally, the study plans to assign malignancy grades to images to aid clinical decision-making for oral diseases.

### Authors Contribution

This work encompasses the development of a comprehensive framework that combines novel deep learning methods, feature extraction techniques, and reduced computational complexity to enhance the detection and classification of oral cancer disorders, ultimately facilitating early diagnosis and improved treatment outcomes.

## References

- Abati, S., Bramati, C., Bondi, S., Lissoni, A., & Trimarchi, M. (2020). Oral cancer and precancer: a narrative review on the relevance of early diagnosis. *International Journal of Environmental Research and Public Health*, 17(24), 9160. <https://doi.org/10.3390/ijerph17249160>
- Alhazmi, A., Alhazmi, Y., Makrami, A., Masmali, A., Salawi, N., Masmali, K., & Patil, S. (2021). Application of artificial intelligence and machine learning for prediction of oral cancer risk. *Journal of Oral Pathology & Medicine*, 50(5), 444-450. <https://doi.org/10.1111/jop.13157>
- Amin, I., Zamir, H., & Khan, F. F. (2021). Histopathological image analysis for oral squamous cell carcinoma classification using concatenated deep learning models. *medRxiv*, 2021-05. <https://doi.org/10.1101/2021.05.06.21256741>
- Ariji, Y., Sugita, Y., Nagao, T., Nakayama, A., Fukuda, M., Kise, Y., Nozawa, M., Nishiyama, M., Katumata, A., & Ariji, E. (2020). CT evaluation of extranodal extension of cervical lymph node metastases in patients with oral squamous cell carcinoma using deep learning classification. *Oral Radiology*, 36, 148-155. <https://doi.org/10.1007/s11282-019-00391-4>
- Bansal, K., Batla, R.K., Kumar, Y., & Shafi, J. (2022). Artificial intelligence techniques in health informatics for oral cancer detection. In *Connected e-Health: Integrated IoT and Cloud Computing*, 255-279. Springer International Publishing. [http://dx.doi.org/10.1007/978-3-030-97929-4\\_11](http://dx.doi.org/10.1007/978-3-030-97929-4_11)
- Bhandari, B., Alsadoon, A., Prasad, P. W. C., Abdullah, S., & Haddad, S. (2020). Deep learning neural network for texture feature extraction in oral cancer: Enhanced loss function. *Multimedia Tools and Applications*, 79(37-38), 27867-27890. Advance online publication. <https://doi.org/10.1007/s11042-020-09384-6>
- Bhandari, B., Alsadoon, A., Prasad, P.W.C., Abdullah, S., & Haddad, S. (2020). Deep learning neural network for texture feature extraction in oral cancer: Enhanced loss function. *Multimedia Tools and Applications*, 79, 27867-27890.
- Capote-Moreno, A., Brabyn, P., Muñoz-Guerra, M.F., Sastre-Pérez, J., Escorial-Hernandez, V., Rodríguez-Campo, F.J., García, T., & Naval-Gías, L. (2020). Oral squamous cell carcinoma: epidemiological study and risk factor assessment based on a 39-year series. *International Journal of Oral and Maxillofacial Surgery*, 49(12), 1525-1534. <https://doi.org/10.1016/j.ijom.2020.03.009>
- Chamoli, A., Gosavi, A.S., Shirwadkar, U.P., Wangdale, K.V., Behera, S.K., Kurrey, N.K., Kalia, K., & Mandoli, A. (2021). Overview of oral cavity squamous cell carcinoma: Risk factors, mechanisms, and diagnostics. *Oral Oncology*, 121, 105451. <https://doi.org/10.1016/j.oraloncology.2021.105451>
- Chu, C.S., Lee, N.P., Adeoye, J., Thomson, P., & Choi, S.W. (2020). Machine learning and treatment outcome prediction for oral cancer. *Journal of Oral Pathology & Medicine*, 49(10), 977-985. <https://doi.org/10.1111/jop.13089>
- Das, D. K., Bose, S., Maiti, A. K., Mitra, B., Mukherjee, G., & Dutta, P. K. (2018). Automatic identification of clinically relevant regions from oral tissue histological images for oral squamous cell carcinoma diagnosis. *Tissue and Cell*, 53, 111-119. <https://doi.org/10.1016/j.tice.2018.06.004>
- Das, N., Hussain, E., & Mahanta, L.B. (2020). Automated classification of cells into multiple classes in epithelial tissue of oral squamous cell carcinoma using transfer learning and convolutional neural network. *Neural Networks*, 128, 47-60. <https://doi.org/10.1016/j.neunet.2020.05.003>
- Deif, M. A., Attar, H., Amer, A., Issa, H., Khosravi, M. R., & Solyman, A. A. A. (2022). A new feature selection method based on a hybrid approach for colorectal cancer histology classification. *Wireless Communications and Mobile Computing*, 2022, Article ID 7614264, 14 pages. <https://doi.org/10.1002/jmri.27599>
- Deshmukh, V., & Shekar, K. (2021). Oral squamous cell carcinoma: Diagnosis and treatment planning. *Oral and maxillofacial surgery for the clinician*, 1853-1867. <https://doi.org/10.3390/diagnostics13071353>

- Dixit, S., Kumar, A., & Srinivasan, K. (2023). A Current Review of Machine Learning and Deep Learning Models in Oral Cancer Diagnosis: Recent Technologies, Open Challenges, and Future Research Directions. *Diagnostics*, *13*(7), 1353.
- El-Hasnony, I.M., Elzeki, O.M., Alshehri, A., & Salem, H. (2022). Multi-label active learning-based machine learning model for heart disease prediction. *Sensors*, *22*(3), 1184. <https://doi.org/10.3390/s22031184>
- Ezhilarasan, D., Lakshmi, T., Subha, M., Deepak Nallasamy, V., & Raghunandhakumar, S. (2022). The ambiguous role of sirtuins in head and neck squamous cell carcinoma. *Oral Diseases*, *28*(3), 559-567. <https://doi.org/10.1111/odi.13798>
- Folmsbee, J., Liu, X., Brandwein-Weber, M., & Doyle, S. (2018, April). Active deep learning: Improved training efficiency of convolutional neural networks for tissue classification in oral cavity cancer. In *2018 IEEE 15th international symposium on biomedical imaging (ISBI 2018)* (pp. 770-773). <https://doi.org/10.1109/ISBI.2018.8363686>
- Fukumoto, C., Uchida, D., & Kawamata, H. (2022). Diversity of the origin of cancer stem cells in oral squamous cell carcinoma and its clinical implications. *Cancers*, *14*(15), 3588. <https://doi.org/10.3390/cancers14153588>
- Huang, C., Zhang, G., Chen, S., & de Albuquerque, V.H.C. (2022). An intelligent multisampling tensor model for oral cancer classification. *IEEE Transactions on Industrial Informatics*, *18*(11), 7853-7861. <https://doi.org/10.1109/TII.2022.3149939>
- Janiesch, C., Zschech, P., & Heinrich, K. (2021). Machine learning and deep learning. *Electronic Markets*, *31*(3), 685-695. <https://doi.org/10.1007/s12525-021-00475-2>
- Jubair, F., Al-karadsheh, O., Malamos, D., Al Mahdi, S., Saad, Y., & Hassona, Y. (2022). A novel lightweight deep convolutional neural network for early detection of oral cancer. *Oral Diseases*, *28*(4), 1123-1130. <https://doi.org/10.1111/odi.13825>
- Ketabat, F., Pundir, M., Mohabatpour, F., Lobanova, L., Koutsopoulos, S., Hadjiiski, L., Chen, X., Papagerakis, P., & Papagerakis, S. (2019). Controlled drug delivery systems for oral cancer treatment—current status and future perspectives. *Pharmaceutics*, *11*(7), 302. <https://doi.org/10.3390/pharmaceutics11070302>
- Khanagar, S.B., Al-Ehaideb, A., Maganur, P.C., Vishwanathaiah, S., Patil, S., Baeshen, H.A., Sarode, S.C., & Bhandi, S. (2021). Developments, application, and performance of artificial intelligence in dentistry—A systematic review. *Journal of dental sciences*, *16*(1), 508-522. <https://doi.org/10.1016/j.jds.2020.06.019>
- Kirubabai, M.P., & Arumugam, G. (2021). Deep learning classification method to detect and diagnose the cancer regions in oral MRI images. *Med. Leg. Update*, *21*, 462-468. <https://doi.org/10.37506/mlu.v21i1.2353>
- Mercadante, V., Scarpa, E., De Matteis, V., Rizzello, L., & Poma, A. (2021). Engineering polymeric nanosystems against oral diseases. *Molecules*, *26*(8), 2229. <https://doi.org/10.3390/molecules26082229>
- Musulini, J., Štifanić, D., Zulijani, A., Čabov, T., Dekanić, A., & Car, Z. (2021). An enhanced histopathology analysis: An AI-based system for multiclass grading of oral squamous cell carcinoma and segmenting of epithelial and stromal tissue. *Cancers*, *13*(8), 1784. <https://doi.org/10.3390/cancers13081784>
- Myriam, H., Abdelhamid, A.A., El-Kenawy, E.S.M., Ibrahim, A., Eid, M.M., Jamjoom, M.M., & Khafaga, D.S. (2023). Advanced meta-heuristic algorithm based on Particle Swarm and Al-biruni Earth Radius optimization methods for oral cancer detection. *IEEE Access*, *11*, 23681-23700. <http://dx.doi.org/10.1109/ACCESS.2023.3253430>
- Panigrahi, S., Nanda, B.S., & Swarnkar, T. (2022). Comparative analysis of machine learning algorithms for histopathological images of oral cancer. In *Advances in Distributed Computing and Machine Learning: Proceedings of ICADCML 2021* (pp. 318-327). Springer Singapore. <http://dx.doi.org/10.1109/ICCPCT58313.2023.10244890>
- Parkavi, A., Tiriyaar, Y., Borthakur, P.J., Patil, P., & Haleem, M.B. (2023, August). Deep Learning Techniques for the Detection and Classification of Oral Cancer Using Histopathological Images. In *2023 International Conference on Circuit Power and Computing Technologies (ICCPCT)* (pp. 1625-1630). IEEE.

- Patibandla, S.K., & Peram, S.R. (2023). CT Image Precise Denoising Model with Edge Based Segmentation with Labeled Pixel Extraction Using CNN Based Feature Extraction for Oral Cancer Detection. *Traitement du Signal*, 40(3), 1297. <https://doi.org/10.18280/ts.400349>
- Rahman, A.U., Alqahtani, A., Aldhafferi, N., Nasir, M.U., Khan, M.F., Khan, M.A., & Mosavi, A. (2022). Histopathologic oral cancer prediction using oral squamous cell carcinoma biopsy empowered with transfer learning. *Sensors*, 22(10), 3833. <https://doi.org/10.3390/s22103833>
- Rao, R.S., Shivanna, D.B., Lakshminarayana, S., Mahadevpur, K.S., Alhazmi, Y.A., Bakri, M.M.H., Alharbi, H.S., Alzahrani, K.J., Alsharif, K.F., Banjer, H.J., & Alnfai, M.M. (2022). Ensemble Deep-Learning-Based Prognostic and Prediction for Recurrence of Sporadic Odontogenic Keratocysts on Hematoxylin and Eosin Stained Pathological Images of Incisional Biopsies. *Journal of Personalized Medicine*, 12(8), 1220. <https://doi.org/10.3390/jpm12081220>
- Shamala, A., Halboub, E., Al-Maweri, S.A., Al-Sharani, H., Al-Hadi, M., Ali, R., Laradhi, H., Murshed, H., Mohammed, M.M., & Ali, K. (2023). Oral cancer knowledge, attitudes, and practices among senior dental students in Yemen: a multi-institution study. *BMC Oral Health*, 23(1), 435. <http://dx.doi.org/10.1186/s12903-023-03149-x>
- Wahid, K.A., Ahmed, S., He, R., van Dijk, L.V., Teuwen, J., McDonald, B.A., Salama, V., Mohamed, A.S., Salzillo, T., Dede, C., & Taku, N. (2022). Evaluation of deep learning-based multiparametric MRI oropharyngeal primary tumor auto-segmentation and investigation of input channel effects: Results from a prospective imaging registry. *Clinical and translational radiation oncology*, 32, 6-14. <https://doi.org/10.1016/j.ctro.2021.10.003>
- Warin, K., Limprasert, W., Suebnukarn, S., Jinaporntham, S., & Jantana, P. (2021). Automatic classification and detection of oral cancer in photographic images using deep learning algorithms. *Journal of Oral Pathology & Medicine*, 50(9), 911-918. <https://doi.org/10.1111/jop.13227>
- Welikala, R., Remagnino, P., Lim, J., Chan, C. S., Rajendran, S., George, T., Zain, R., Jayasinghe, R., Rimal, J., Kerr, A., Amtha, R., Patil, K., Tilakaratne, W., Gibson, J., Cheong, S., & Barman, S. (2020). Automated Detection and Classification of Oral Lesions Using Deep Learning for Early Detection of Oral Cancer. *IEEE Access*, 8, 1-1. <http://dx.doi.org/10.1109/ACCESS.2020.3010180>
- Zhou, Y., Tang, Y., Luo, J., Yang, Y., Zang, H., Ma, J., Fan, S. and Wen, Q., (2023). High expression of HSP60 and survivin predicts poor prognosis for oral squamous cell carcinoma patients. *BMC Oral Health*, 23(1), p.629. <https://doi.org/10.1186/s12903-023-03311-5>